Observation of flat electron temperature profiles in the Lithium Tokamak Experiment

D.P. Boyle,[1,*] R. Kaita,[1] R. Majeski,[1] C. Hansen,[2] S. Kubota,[3] J.C. Schmitt,[4] and M. Lucia[1]

[1] *Princeton Plasma Physics Laboratory, Princeton, New Jersey 08543, USA*

[2] *PSI-Center, University of Washington, Seattle, Washington 98195, USA*

[3] *Institute of Plasma and Fusion Research, University of California, Los Angeles, California 90095*

[4] *Physics Department, Auburn University, Auburn, Alabama 36849, USA*

(Dated: September 13, 2016)

Abstract

It has been predicted for over a decade that low-recycling plasma facing components in fusion devices would lead to high edge temperatures and flat or nearly flat temperature profiles. In recent experiments with lithium wall-coatings in the Lithium Tokamak Experiment (LTX), a hot edge (> 200 eV) and flat electron temperature profiles have been measured following the termination of external fueling. Reduced recycling is demonstrated by retention of $\sim 60\%$ of the injected hydrogen in the walls following the discharge. Achievement of the low-recycling, hot edge regime has been an important goal of LTX and Li PFC research in general, as it has far-reaching implications for the operation, design, and cost of fusion devices.

PACS numbers:

The use of lithium as a wall material in fusion devices has the potential to enable a fundamentally different operating regime than the conventional approach based on high-recycling, high-density, low-temperature detached divertors. By chemically bonding hydrogen isotopes, lithium (Li) can reduce wall-recycling and edge neutral density, and thus has been predicted to allow low edge densities and high edge temperatures with flat or nearly flat temperature profiles. Avoiding the low edge temperature boundary condition imposed by the influx of cold neutrals is expected to suppress temperature gradient driven instabilities and improve confinement [1, 2]. Improved confinement would enable more compact fusion devices with lower capital cost, and lithium walls could also reduce risks of costly downtime and repairs to the plasma facing components (PFCs). While the conventional high-density, low-temperature divertor concept is motivated by spreading heat loads to avoid thermal damage to solid materials and reduce erosion and impurity influx by sputtering [], lithium would naturally be liquid in a fusion device, making it robust to damage with the ability to handle large heat loads. Lithium is also attractive because of its low first ionization potential, meaning sputtered Li will ionize close to the wall and redeposit rather than entering the confined plasma as an impurity. Lithium's low atomic number $Z = 3$ also means relatively large Li impurity concentrations would be tolerable in a fusion device. While at low edge temperatures, material sputtering increases with edge temperature, sputtering yield for Li peaks at $T_e \sim 200$ eV and then decreases with edge temperature [3], making a high-temperature, low-density edge feasible with a lithium wall.

Experiments using lithium coated surfaces have shown a variety of performance improvements, mainly attributed to reduced recycling. Improved density control and H/D ratio were achieved due to pumping of the dominant plasma species by Li []. The National Spherical Torus Experiment (NSTX) demonstrated higher edge rotation, likely because Li reduced neutrals and therefore charge exchange drag [4]. NSTX and the Experimental Advanced Superconducting Tokamak (EAST) [5] also saw suppression of edge-localized modes (ELMs), explained in NSTX by the change in recycling that modified pedestal profiles and therefore the bootstrap current [6, 7]. Li coatings also led to greatly improved confinement in Tokamak Fusion Test Reactor (TFTR) [8], Current Drive Experiment-Upgrade (CDX-U) [9], NSTX [], and Doublet III-Divertor (DIII-D) [10]. In TFTR, the improved confinement was associated with reduced turbulence [11].

The LTX device is a spherical tokamak [12] designed and built specifically to study Li

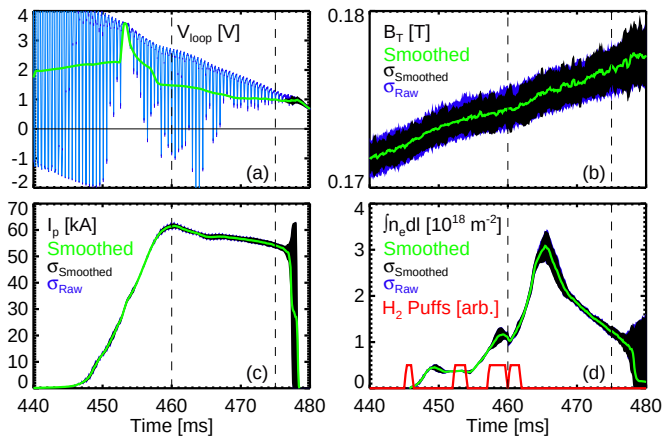

FIG. 1. Waveforms of (a) loop voltage V_{loop}, (b) toroidal field B_T, (c) plasma current I_p, and (d) line-integrated density $\int n_e d\ell$. The green line is the median over the 55 discharges of the time-smoothed waveforms, the black band is the standard deviation of the smoothed waveforms, and the blue band is the standard deviation of the raw waveforms. The gas puffing is overlaid in (d) as a red line.

PFCs [13]. In early experiments using neutral helium to disperse solid Li coatings, significant improvement in performance was shown. Neutral pressure and residual gas analyzer measurements showed high pumping and retention of the fueling gas [14, 15], and lowered recycling was inferred from Lyman-α measurements and interpretive modeling with the DEGAS2 neutrals code [16, 17]. Later experiments with electron-beam evaporation showed additional improvements, including good performance using liquid lithium coatings [18, 19]. Using the Materials Analysis and Particle Probe (MAPP) to make *in vacuo* measurements, it was determined that while the surface was mostly oxidized within a few hours, the solid lithium coatings were still effective at pumping hydrogen [20–22].

In the LTX vacuum vessel, a close fitting shell surrounds $\sim$ 80% of the plasma surface, with toroidal and poloidal breaks dividing the shell into 4 quadrants. The shell is 1 cm copper with a 1.5 mm stainless steel liner providing a lithium-compatible PFC. For the experiments described here, $\sim$ 150-200 mg of Li was evaporated from each side, giving coatings $\sim$ 75-100 nm thick assuming uniform coverage. The shell was allowed to cool overnight and discharges were performed the following day.

A series of 55 reproducible discharges were repeated with identical programming during a single run day (Figure 1). As the LTX Thomson scattering system [23, 24] can measure

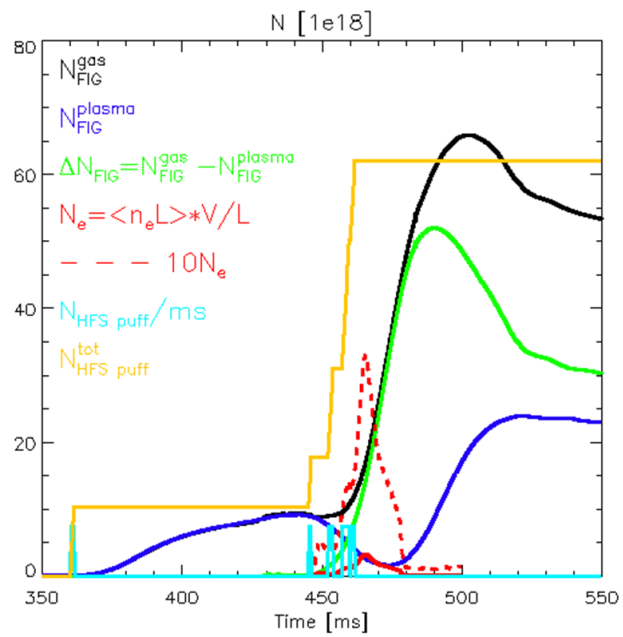

FIG. 2. Neutral hydrogen atom inventory from fast ion gauge waveform without plasma (black), with plasma (blue), and the difference (green). Electron inventory from interferometer and reconstructed plasma geometry (red), and scaled by 10 (dashed red). Fueling rate from high-field side gas puffer (aqua) and integrated fueling (orange).

electron density and temperature profiles only once per discharge, repeated discharges were necessary to measure time evolution of the plasma profiles. The vessel was prefilled with 8×10^5 Torr of H_2, and breakdown occurred at $\sim$ 445 ms. The pre-programmed waveform of the ohmic heating central solenoid induced the plasma current (I_p) with a peak value of $\sim$ 60 kA at 460 ms that decreased slightly over the next $\sim$ 17 ms before the discharge terminated. Additional fueling was provided from the high field side puffer, including a large puff at the I_p peak. There was no additional fueling after the I_p peak, allowing study of the plasma with recycling as the only source of neutral gas.

As Li readily pumps hydrogen atoms and ions, but not molecular hydrogen, one simple indicator of reduced recycling due to the Li coatings is the reduction in vessel neutral pressure after the discharges terminated, relative to calibration shots taken throughout the day with identical gas fueling but no plasma [14, 15]. In Figure 2, the black curve shows the averaged neutral pressure for the gas-only shots, as measured with a vessel fast-ion gauge, while the blue curve shows the averaged neutral pressure for the plasma discharges. During the

discharge, the neutral pressure is greatly reduced as the particles are confined in the plasma volume and retained in the walls. When the discharge terminates, the plasma recombines to molecular hydrogen, and in the absence of wall retention, the vessel pressure would return to the gas-only value. The difference in vessel pressure between the gas-only and plasma shots, shown in green, gives the amount of hydrogen retained in the walls, equivalent to 60% of the hydrogen puffed to fuel the plasma.

Thomson scattering (TS) is the key diagnostic in the present study. The LTX TS ruby laser fires a single 15-20 J, $\sim$ 35 ns FMHW pulse per discharge on a near-radial midplane path [23, 24]. Light is imaged using downward viewing optics onto an array of optical fibers and 11 channels covering the outboard radial midplane are measured with a spectrometer and intensified camera. The TS measurement time was varied over the 55 repeated discharges in 1 ms intervals covering the period from 460-477 ms, with measurements at each time point repeated several times. In order to improve signal-to-noise, the raw spectra were averaged for all TS measurements taken at the same time point, as well as their nearest neighbors in time. The measurement time of averaged spectra was taken to be the average of the the measurement times. The TS density (n_e) profiles were mapped to the high field side of the magnetic axis, fit with smoothing splines, numerically integrated, and normalized to the line integrated density $\int n_e d\ell$ measured with a 1 mm microwave interferometer [25] on a radial midplane path reflected off the center stack. For an initial normalization, the mapping was performed based on the plasma boundary as determined with flux loops and mirnov coils [] and an analytic formula for the Shafranov shift [26]. The TS profiles of electron pressure p_e, and an assumption for ion pressure $p_i = 0.3p_e$ were used to constrain magnetic equilibrium reconstructions using PSI-TRI. PSI-TRI is an axisymmetric equilibrium code that includes a model for eddy currents induced in the thick copper shell as well as the vacuum vessel [27, 28]. Final n_e normalizations using the magnetic reconstructions for mapping were only slightly changed from the initial normalizations.

Figure 3 shows n_e, T_e, and p_e profiles near the peak density from the large gas puff at t = 465 ms (left) and long after external gas fueling was terminated at t = 474 ms (right). Though 11 radial points were measured, the three farthest outboard were unreliable due to low count rates and are not shown. The accuracy of the TS profiles are corroborated by comparison of the n_e profiles with those measured with a profile reflectometer [29]. The major radii of magnetic axis and LCFS at the outer midplane are shown as vertical lines,

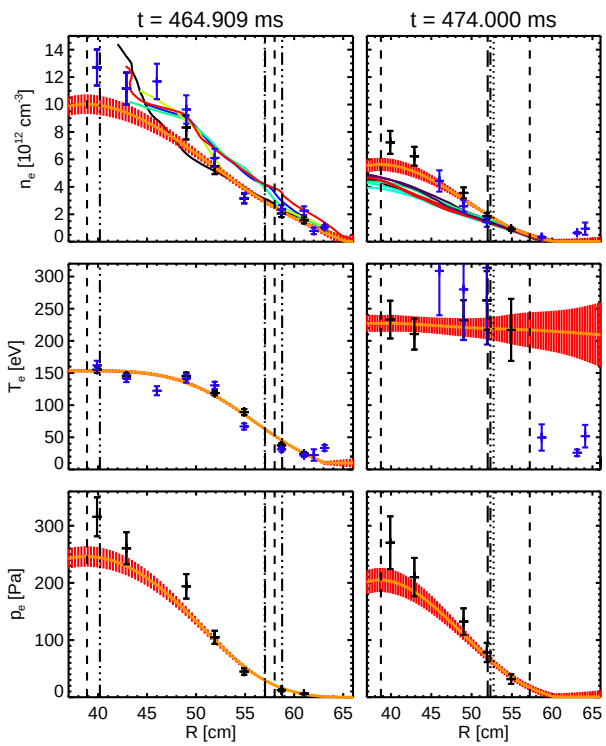

FIG. 3. TS n_e, T_e, and p_e profiles (black) and smoothing spline fits (red) during the peak of the gas puff (left) and after fueling ceased (right). The magnetic axis and LCFS from magnetic reconstructions are shown as vertical dashed lines. Reflectometer n_e profiles are overlaid on the TS n_e profiles. Black TS points - time smoothed as in thesis. Blue TS only at actual time point, less spectra to average so worse statistics but less variation from time evolution. Solid lines - reflectometer profiles, Black: -1 ms, Dark Blue: -0.5 ms, Light Blue: given time, Green +0.5 ms, Yellow +1 ms, Vertical dashed: axis and LCFS; - - - TS PSITRI _ _ _ John Rmidout ... John bdry shape -...- Mag PSITRI

calculated using the PSI-TRI equilibria and the flux loop measurements.

The determination of the last closed flux surface (LCFS) in LTX has some uncertainties, but the observation that the T_e profile remains flat from the core to the edge after external fueling is terminated is robust to several different methods of interpretation. Later in the discharge, the radius of the outboard midplane LCFS determined solely using magnetics is $\sim$ 5 cm less than that determined using the TS constrained reconstruction. This difference means that T_e remains above 200 eV for 2-3 cm beyond the plasma edge at the LCFS determined using the magnetics only measurement, while the farthest outboard point is

still 2 cm inside the TS constrained boundary measurement. The TS and reflectometer both show a gradually decreasing n_e profile, with no evidence of the sharp edge density gradient seen in the standard high-confinement regime (the H-mode pedestal). Based on the TS constrained LCFS measurement, a sharp temperature drop inside the LCFS cannot be completely excluded. However, a hypothetical T_e pedestal would imply a transport barrier that confines energy but not particles such as I-mode [30], which has not been previously observed in a tokamak operating without auxiliary heating, at low aspect ratio, or with a limiter rather than a divertor.

Given the longstanding predictions of flat temperature profiles with low recycling PFCs, the confirmation of the predictions is striking. The dramatic change in the T_e profile from peaked to flat following the termination of external fueling suggests that the PFCs did not continue to provide a steady source of cold neutrals, but rather retained hydrogen, as independently measured by the fast ion gauge. The achievement of such flat T_e profiles was a major goal of LTX and gives evidence for a new, potentially high performance plasma regime for fusion devices. This regime will be studied further in the upcoming LTX-β, which will include the addition of a neutral beam. Core fueling with a neutral beam will provide auxiliary heating and allow the density to remain stationary in the low recycling regime without edge fueling .

* dboyle@pppl.gov

[1] S. I. Krasheninnikov, L. E. Zakharov, and G. V. Pereverzev, Physics of Plasmas **10**, 1678 (2003).

[2] L. E. Zakharov, N. Gorelenkov, R. White, S. I. Krasheninnikov, and G. V. Pereverzev, Fusion Engineering and Design **72**, 149 (2004).

[3] J. Laszlo and W. Eckstein, Journal of Nuclear Materials **184**, 22 (1991).

[4] D. K. Mansfield, H. W. Kugel, R. Maingi, M. G. Bell, R. E. Bell, R. Kaita, J. Kallman, S. M. Kaye, B. P. LeBlanc, and D. Mueller, Journal of Nuclear Materials **390-391**, 764 (2009).

[5] J. Li, H. Y. Guo, B. N. Wan, X. Z. Gong, Y. F. Liang, G. S. Xu, K. F. Gan, J. S. Hu, H. Q. Wang, L. Wang, L. Zeng, Y. P. Zhao, P. Denner, G. L. Jackson, A. Loarte, R. Maingi, J. E. Menard, M. Rack, and X. L. Zou, Nature Physics **9**, 817 (2013).

[6] D. P. Boyle, R. Maingi, P. B. Snyder, J. Manickam, T. H. Osborne, R. E. Bell, and B. P. LeBlanc, Plasma Physics and Controlled Fusion **53**, 105011 (2011).

[7] R. Maingi, S. M. Kaye, C. H. Skinner, D. P. Boyle, J. M. Canik, M. G. Bell, R. E. Bell, T. K. Gray, M. A. Jaworski, R. Kaita, H. W. Kugel, B. P. LeBlanc, D. K. Mansfield, T. H. Osborne, S. A. Sabbagh, and V. A. Soukhanovskii, Physical Review Letters **107**, 145004 (2011).

[8] D. K. Mansfield, K. W. Hill, J. D. Strachan, M. G. Bell, S. D. Scott, R. Budny, E. S. Marmar, J. A. Snipes, J. L. Terry, S. Batha, R. E. Bell, M. Bitter, C. E. Bush, Z. Chang, D. S. Darrow, D. Ernst, E. D. Fredrickson, B. Grek, H. W. Herrmann, A. Janos, D. L. Jassby, F. C. Jobes, D. W. Johnson, L. C. Johnson, F. M. Levinton, D. R. Mikkelsen, D. Mueller, D. K. Owens, H. K. Park, A. T. Ramsey, A. L. Roquemore, C. H. Skinner, T. N. Stevenson, B. C. Stratton, E. J. Synakowski, G. Taylor, A. von Halle, S. von Goeler, K. L. Wong, and S. J. Zweben, Physics of Plasmas **3**, 1892 (1996).

[9] R. Majeski, R. P. Doerner, T. Gray, R. Kaita, R. Maingi, D. K. Mansfield, V. A. Soukhanovskii, J. Spaleta, J. Timberlake, and L. E. Zakharov, Physical Review Letters **97**, 075002 (2006).

[10] T. Osborne, G. Jackson, Z. Yan, R. Maingi, D. Mansfield, B. Grierson, C. Chrobak, a.G. McLean, S. Allen, D. Battaglia, a.R. Briesemeister, M. Fenstermacher, G. McKee, and P. Snyder, Nuclear Fusion **55**, 063018 (2015).

[11] D. R. Ernst, B. Coppi, S. D. Scott, and M. Porkolab, Physical Review Letters **81**, 2454 (1998).

[12] M. Ono and R. Kaita, Physics of Plasmas **22**, 040501 (2015).

[13] R. Majeski, L. Berzak, T. Gray, R. Kaita, T. Kozub, F. M. Levinton, D. Lundberg, J. Manickam, G. V. Pereverzev, K. Snieckus, V. A. Soukhanovskii, J. Spaleta, D. Stotler, T. Strickler, J. Timberlake, J. Yoo, and L. E. Zakharov, Nuclear Fusion **49**, 055014 (2009).

[14] D. P. Lundberg, *Princeton University*, Ph.D. thesis, Princeton University (2012).

[15] J. C. Schmitt, T. Abrams, L. R. Baylor, L. B. Hopkins, T. Biewer, D. Bohler, D. Boyle, E. Granstedt, T. Gray, J. Hare, C. M. Jacobson, M. Jaworski, R. Kaita, T. Kozub, B. Leblanc, D. P. Lundberg, M. Lucia, R. Maingi, R. Majeski, E. Merino, A. Ryou, E. Shi, J. Squire, D. Stotler, C. E. Thomas, K. Tritz, and L. Zakharov, Journal of Nuclear Materials **438**, S1096 (2013).

[16] E. M. Granstedt, *Princeton University*, Ph.D. thesis, Princeton University (2013).

[17] D. Stotler and C. Karney, Contributions to Plasma Physics **34**, 392 (1994).

[18] K. Tritz, R. E. Bell, P. Beiersdorfer, D. Boyle, J. Clementson, M. Finkenthal, R. Kaita, T. Kozub, S. Kubota, M. Lucia, R. Majeski, E. Merino, J. Schmitt, and D. Stutman, Plasma Physics and Controlled Fusion **56**, 125014 (2014).

[19] J. C. Schmitt, R. E. Bell, D. P. Boyle, B. Esposti, R. Kaita, T. Kozub, B. P. LeBlanc, M. Lucia, R. Maingi, R. Majeski, E. Merino, S. Punjabi-Vinoth, G. Tchilingurian, A. Capece, B. Koel, J. Roszell, T. M. Biewer, T. K. Gray, S. Kubota, P. Beiersdorfer, K. Widmann, and K. Tritz, Physics of Plasmas **22**, 056112 (2015).

[20] M. J. Lucia, *Princeton University*, Ph.D. thesis, Princeton University (2015).

[21] M. Lucia, R. Kaita, R. Majeski, F. Bedoya, J. Allain, T. Abrams, R. Bell, D. Boyle, M. Jaworski, and J. Schmitt, Journal of Nuclear Materials **463**, 907 (2015).

[22] R. Kaita, M. Lucia, J. P. Allain, F. Bedoya, R. Bell, D. Boyle, A. Capece, M. Jaworski, B. E. Koel, R. Majeski, J. Roszell, J. Schmitt, F. Scotti, C. H. Skinner, and V. Soukhanovskii, Fusion Engineering and Design (2016), 10.1016/j.fusengdes.2016.06.056.

[23] T. Strickler, R. Majeski, R. Kaita, and B. P. LeBlanc, Review of Scientific Instruments **79**, 10E738 (2008).

[24] C. M. Jacobson, *Princeton University*, Ph.D. thesis, Princeton University (2014).

[25] L. Porte, C. L. Rettig, W. a. Peebles, and X. Ngyuen, Review of Scientific Instruments **70**, 1082 (1999).

[26] J. P. Freidberg, *Ideal Magnetohydrodynamics* (Plenum Press, 1987).

[27] C. J. Hansen, *University of Washington*, Ph.D. thesis, University of Washington (2014).

[28] C. J. Hansen, T. Benedett, A. Hossack, T. Jarboe, J. Levesque, and J. Schmitt, in *Workshop on Exploratory Topics in Plasma and Fusion Research* (Auburn, AL, 2016).

[29] S. Kubota, X. V. Nguyen, W. A. Peebles, L. Zeng, E. J. Doyle, and A. L. Roquemore, Review of Scientific Instruments **72**, 348 (2001).

[30] D. Whyte, a.E. Hubbard, J. Hughes, B. Lipschultz, J. Rice, E. Marmar, M. Greenwald, I. Cziegler, a. Dominguez, T. Golfinopoulos, N. Howard, L. Lin, R. McDermott, M. Porkolab, M. Reinke, J. Terry, N. Tsujii, S. Wolfe, S. Wukitch, and Y. Lin, Nuclear Fusion **50**, 105005 (2010).